Journal of the American College of Cardiology
© 2006 by the American College of Cardiology Foundation
Published by Elsevier Inc.

Vol. 48, No. 1, 2006
ISSN 0735-1097/06/$32.00
doi:10.1016/j.jacc.2006.04.008

PRECLINICAL STUDY

Erythropoietin Enhances Neovascularization of Ischemic Myocardium and Improves Left Ventricular Dysfunction After Myocardial Infarction in Dogs

Akio Hirata, MD,* Tetsuo Minamino, MD, PHD,* Hiroshi Asanuma, MD, PHD,* Masashi Fujita, MD,* Masakatsu Wakeno, MD,† Masafumi Myoishi, MD,† Osamu Tsukamoto, MD,* Ken-ichiro Okada, MD,* Hidekazu Koyama, BS,* Kazuo Komamura, MD, PHD,§ Seiji Takashima, MD, PHD,* Yoshiro Shinozaki, MD,‖ Hidezo Mori, MD, PHD,§ Masamichi Shiraga, MD, PHD,‡ Masafumi Kitakaze, MD, PHD, FACC,§ Masatsugu Hori, MD, PHD, FACC*

Osaka and Kanagawa, Japan

OBJECTIVES We investigated the effects of erythropoietin (EPO) on neovascularization and cardiac function after myocardial infarction (MI).

BACKGROUND Erythropoietin exerts antiapoptotic effects and mobilizes endothelial progenitor cells (EPCs).

METHODS We intravenously administered EPO (1,000 IU/kg) immediately [EPO(0) group], 6 h [EPO(6h) group], or 1 week [EPO(1wk) group] after the permanent ligation of the coronary artery in dogs. Control animals received saline immediately after the ligation.

RESULTS The infarct size 6 h after MI was significantly smaller in the EPO(0) group than in the control group (61.5 ± 6.0% vs. 22.9 ± 2.2%). One week after MI, the circulating CD34-positive mononuclear cell numbers in both the EPO(0) and the EPO(6h) groups were significantly higher than in the control group. In the ischemic region, the capillary density and myocardial blood flow 4 weeks after MI was significantly higher in both the EPO(0) and the EPO(6h) groups than in the control group. Four weeks after MI, left ventricular (LV) ejection fraction in the EPO(6h) (48.6 ± 1.9%) group was significantly higher than that in either the control (41.9 ± 0.9%) or the EPO(1wk) (42.6 ± 1.2%) group but significantly lower than that in the EPO(0) group (56.1 ± 2.3%). The LV end-diastolic pressure 4 weeks after MI in both the EPO(0) and the EPO(6h) groups was significantly lower than either the control or the EPO(1wk) group. Hematologic parameters did not differ among the groups.

CONCLUSIONS In addition to its acute infarct size-limiting effect, EPO enhances neovascularization, likely via EPC mobilization, and improves cardiac dysfunction in the chronic phase, although it has time-window limitations. (J Am Coll Cardiol 2006;48:176–84) © 2006 by the American College of Cardiology Foundation

Erythropoietin (EPO) is a cytokine that promotes proliferation and differentiation of erythroid precursor cells (1) and is widely used for the treatment of anemia in patients with chronic renal failure (2). Erythropoietin can also exert antiapoptotic and radical scavenger effects on nonerythroid cells (3,4). Indeed, we and others showed that an administration of EPO before or shortly after the onset of ischemia

See page 185

reduced myocardial infarct size and improved cardiac function in acute phases (5–8). Another interesting nonerythroid function of EPO is the promotion of endothelial progenitor cell (EPC) mobilization in animals and humans (9–11), which may enhance neovascularization of ischemic areas (12,13). We hypothesized that EPO increases blood supply to ischemic regions through promoting neovascularization and improves cardiac dysfunction after ischemic insult. Thus, the goal of this study was to characterize the effects of EPO on neovascularization and cardiac function after myocardial infarction (MI) in the chronic phase.

METHODS

All procedures were performed in conformity with the Guide for the Care and Use of Laboratory Animals (NIH publication no. 85-23, 1996 revision) and were approved by the Osaka University Committee for Laboratory Animal Use.

Instrumentation. Forty-seven beagle dogs (Kitayama Labes, Yoshiki Farm Gifu, Japan), weighing 8 to 12 kg were used in these experiments. After an intravenous injection of sodium pentobarbital (15 mg/kg), the dogs were intubated and ventilated. General anesthesia was maintained with 0.5% to 2.0% inhaled isoflurane. After baseline echocardiography and hemodynamic assessment, minimal thoracot-

From the Departments of *Cardiovascular Medicine, †Bioregulatory Medicine, and ‡Hematology and Oncology, Osaka University Graduate School of Medicine, Suita, Osaka, Japan; §Cardiovascular Division of Internal Medicine, National Cardiovascular Center, Suita, Osaka, Japan; and the ‖Department of Physiological Science, Tokai University School of Medicine, Isehara, Kanagawa, Japan.

Manuscript received June 14, 2005; revised manuscript received November 10, 2005, accepted November 30, 2005.

Abbreviations and Acronyms

ABP	= arterial mean blood pressure
Dil-ac-LDL	= 1,1′-dioctadecyl-3,3,3′,3′-tetramethylindocarbocyanine-labeled acetylated low density lipoprotein
EPC	= endothelial progenitor cell
EPO	= erythropoietin
HR	= heart rate
LAD	= left anterior descending coronary artery
LCX	= left circumflex coronary artery
LV	= left ventricle/ventricular
LVEDD	= left ventricular end-diastolic dimension
LVEDP	= left ventricular end-diastolic pressure
MBF	= myocardial blood flow
MI	= myocardial infarction
MNC	= mononuclear cell
UEA-I	= *Ulex europaeus* agglutinin I
VEGF	= vascular endothelial growth factor

omy was performed, and then the left anterior descending coronary artery (LAD) was ligated just distal to the first diagonal branch. To ensure that all animals included in the data analysis were exposed to a similar extent of ischemia, animals with excessive myocardial collateral blood flow (>15 ml/100 g/min) were excluded from study as previously described (14).

Experimental protocols. ACUTE EFFECTS OF EPO ON MYOCARDIAL INFARCT SIZE. Either a single dose of EPO (1,000 IU/kg; 5 ml) (n = 6) or the same volume of saline (n = 6) was administered intravenously immediately after the LAD ligation. Regional myocardial blood flow (MBF), area at risk, and infarct size at 6 h after the LAD ligation were determined as described previously (Fig. 1) (14). Recombinant human EPO was provided by Chugai Pharmaceutical Co. Ltd. (Tokyo, Japan). Recombinant human EPO is effective for correcting anemia in the beagle dog (15).

EFFECTS OF IMMEDIATE OR DELAYED TREATMENT WITH EPO ON NEOVASCULARIZATION AND CARDIAC FUNCTION. A single dose of EPO (1,000 IU/kg; 5 ml) was administered intravenously immediately [EPO(0) group, n = 8], 6 h [EPO(6h) group, n = 8], or 1 week [EPO(1wk) group, n = 7] after the LAD ligation. Control animals received the same volume of saline (control group, n = 8) immediately after the LAD ligation.

Hematologic parameters. Blood was sampled from a peripheral vein under pentobarbital (15 mg/kg) anesthesia at the time points indicated in Figure 2. Hematologic parameters, including hematocrit, white blood cell count, and platelet count, were measured.

Cytokine measurements. Plasma levels of vascular endothelial growth factor (VEGF) were measured by enzyme-linked immunosorbent assay (R & D Systems, Minneapolis, Minnesota). The detection limit of the assays was 9 pg/ml. The reliability of this assay in dogs has already been reported previously (16).

Quantification of CD34-positive mononuclear cells. The circulating CD34-positive mononuclear cells (CD34+MNCs) were quantified at the time points indicated in Figure 2. In brief, peripheral white blood cells were stained with a phycoerythrin-conjugated anticanine CD34 monoclonal antibody (BD Pharmingen, San Diego, California). Samples were then subjected to a two-dimensional side-scatter-fluorescence dot plot analysis (FACScan, Becton-Dickinson, Tokyo, Japan). After appropriate gating of

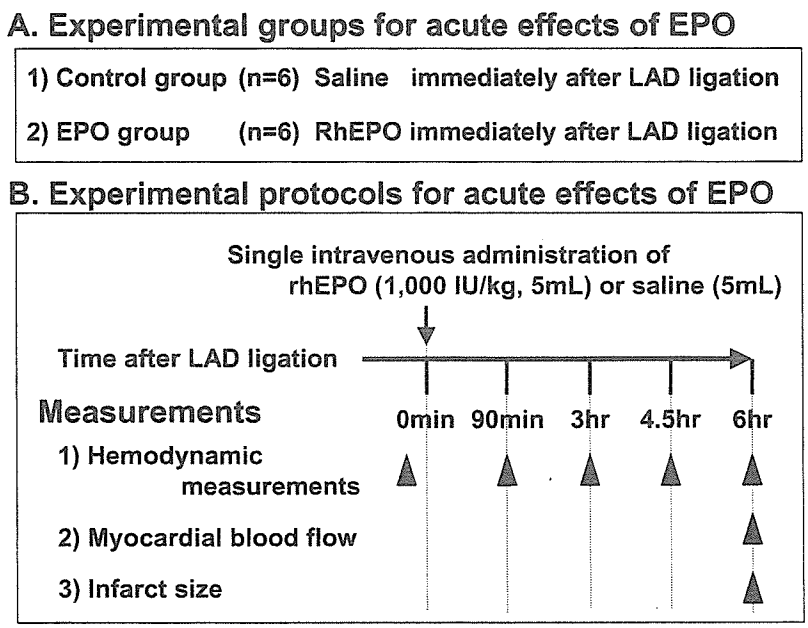

Figure 1. Experimental protocols to investigate acute effects of erythropoietin (EPO) on myocardial infarct size. LAD = left anterior descending coronary artery; RhEPO = recombinant human erythropoietin.

JACC Vol. 48, No. 1, 2006
July 4, 2006:176–84

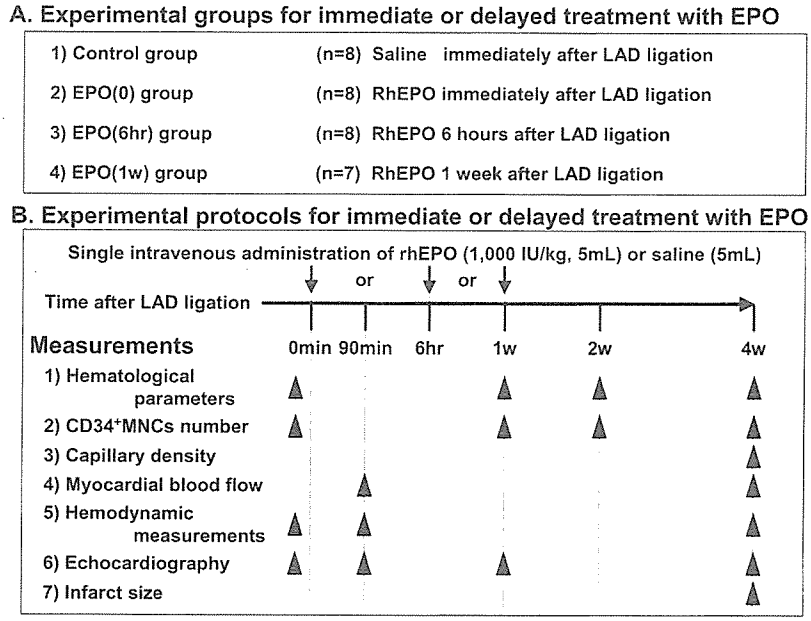

Figure 2. Experimental protocols to investigate effects of immediate or delayed treatment with erythropoietin (EPO) on neovascularization and cardiac function. CD34+MNC = CD34-positive mononuclear cell; other abbreviations as in Figure 1.

MNCs, the number of CD34+MNCs with low cytoplasmic granularity (low sideward scatter) was quantified and expressed as the number of cells per 1-μl blood sample.

In vitro MNC culture assay. Circulating MNCs were isolated from blood (10 ml) of dogs at baseline and 1 week after MI in the control and EPO(0) groups (n = 4 each) by Ficoll density-gradient centrifugation. After MNCs (107 per well) were plated in Medium 199 (Gibco, Grand Island, New York) supplemented with 20% fetal calf serum and antibiotics on human fibronectin-coated six-well dishes. After 7 days in culture, adherent cells were stained for the uptake of 1,1′-dioctadecyl-3,3,3′,3′-tetramethylindocarbocyanine-labeled acetylated low-density lipoprotein (DiI-ac-LDL) (Biomedical Technologies, Stoughton, Massachusetts) and the binding of fluorescein isothiocyanate-labeled *Ulex europaeus* agglutinin I (UEA-I) (Vector Laboratories, Peterborough, England). Double-staining cells were quantified by examining five random microscopic fields (×200 power) (10,11).

Histologic assessments. Four weeks after MI, myocardial tissue was sampled from both ischemic (LAD) and nonischemic (left circumflex coronary artery [LCX]) regions in each group. The tissues in the ischemic region were identified as the edge of the region showing necrosis. These samples were then fixed in 10% buffered formalin, embedded in paraffin, and serially sectioned in the frontal plane at 5-μm thickness. Endothelial cells were immunohistologically stained using rabbit antihuman von Willebrand factor antibody (Dako, Kyoto, Japan) and the Envision+/HRP Kit (Dako) (17). The peroxidase was visualized by incubation with 3,3'-diaminobenzidine, followed by incubation with a DAB-enhancing solution (Dako). We counted the numbers of capillaries and cardiomyocytes in 20 random high-power fields (×400 power), and then calculated the average capillary density and capillary-to-myocyte ratio (18).

Measurements of regional MBF. Regional MBF was determined as described previously (19). Nonradioactive microspheres (Sekisui Plastic Co., Tokyo, Japan) made of inert plastic were labeled with bromine or niobium. Microspheres were administered at 90 min and 4 weeks after MI. The MBF in the LAD region was calculated according to the following formula: time flow = (tissue count) × (reference flow)/(reference count), and was expressed in ml/g wet weight/min.

Hemodynamic measurements. Hemodynamic parameters, such as arterial mean blood pressure (ABP), heart rate (HR), and left ventricular end-diastolic pressure (LVEDP), were measured at the time points indicated in Figure 2. A 5-F sidearm sheath (Radifocus, Terumo, Tokyo, Japan) was placed in the right femoral artery for hemodynamic measurements. A 4-F pigtail catheter (Outlook, Terumo) was placed in the LV for measurement of LVEDP and was connected to a pressure transducer (model DX-200, Nihon Kohden, Tokyo, Japan). The ABP and HR were monitored via the 5-F sidearm sheath.

Echocardiography. Cardiac function was assessed by echocardiography (Sonos 5500, S4-probe, 2-4 MHz, Philips, Bothell, Washington) at the time points indicated in Figure 2. Short-axis views were recorded at the level of midpapillary muscles, and two-dimensional and M-mode views were recorded at the same level. Measurements of left ventricular end-diastolic dimension (LVEDD) and LV ejection fraction were obtained from M-mode views. All measurements were made by one observer, who was blinded with respect to the identity of the tracings.

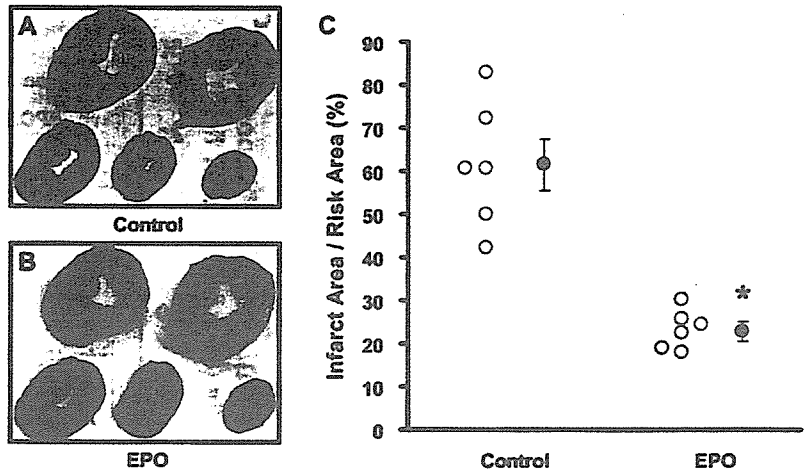

Figure 3. Representative left ventricular cross sections at 6 h after myocardial infarction (MI) in dogs with **(B)** and without **(A)** erythropoietin (EPO) treatment. **(C)** Infarct size at 6 h after MI. *p < 0.05 vs. the control group. **Open circles** = infarct size in each animal.

Infarct size 4 weeks after MI. Myocardial infarct area was determined at the end of the protocol by triphenyltetrazolium chloride staining as described previously (14). Infarct size was expressed as a percentage of the total LV area.

Statistical analysis. Results are expressed as the mean ± standard error of the mean. Comparisons of the time course of the change between groups were performed using two-way repeated measures analysis of variance. Comparisons of other data between groups were performed using one-way factional analysis of variance. If statistical significance was found for a group, a time effect, or a group-by-time interaction, further comparisons were made with paired *t* tests between all possible pairs of four groups at individual time points. The Bonferroni-Holm procedure was used for correction of multiple comparisons. A p value <0.05 was considered to represent statistical significance (20).

RESULTS

Exclusion. Four dogs [acute effects protocol; control: 1, EPO: 0, delayed treatment effects protocol; control: 1, EPO(0): 1, EPO(6h): 0, EPO(1wk): 1] were excluded from analysis because of excessive regional MBF (>15 ml/100 g/min). Thus, 12 and 31 dogs in acute and delayed EPO treatment protocols, respectively, were included.

Acute effects of EPO on infarct size. Myocardial infarct size was significantly smaller in animals receiving EPO compared with those that received saline, but there was no significant difference in regional MBF (9.0 ± 1.0 ml/100 g/min vs. 8.5 ± 1.2 ml/100 g/min) or area at risk (42.9 ± 2.3% vs. 42.3 ± 0.9%) when comparing the two groups (Fig. 3).

Effects of EPO on hematologic parameters. The average change in hematologic parameters was not different when comparing the three EPO-treated groups and the control group over the 4-week experimental protocol (Table 1).

Plasma VEGF levels. Table 2 shows the time course of changes in plasma VEGF level after MI. The plasma VEGF level was significantly and comparably elevated in both control and EPO(0) groups, peaking on 6 h after MI, and returned to baseline at 1 week after MI.

Circulating CD34+MNCs and in vitro cultured MNCs. Figure 4A shows the time course of changes in circulating CD34+MNC number in the different groups. One week after MI, the number of circulating CD34+MNCs increased in all groups. Furthermore, the number of circulating CD34+MNCs at 1 week after MI was higher in the EPO(0) and EPO(6h) groups than in either control or EPO(1wk) group. Two weeks after MI, the number of CD34+MNCs in the control group returned to the baseline. By contrast, the number of CD34+MNCs in the EPO(0) and EPO(6h) groups also decreased but still remained higher than those in either the control or

Table 1. Time Course of Changes in Hematologic Parameters

Parameters	Baseline	1 Week	2 Weeks	4 Weeks
Hematocrit (%)				
Control	52.9 ± 1.7	47.0 ± 1.6	48.9 ± 2.3	53.1 ± 1.8
EPO(0)	52.4 ± 1.1	48.2 ± 1.2	47.9 ± 1.4	53.4 ± 0.7
EPO(6h)	51.5 ± 1.6	49.3 ± 1.6	51.4 ± 1.1	51.3 ± 2.3
EPO(1wk)	48.9 ± 1.0	46.4 ± 1.1	49.4 ± 0.5	50.1 ± 1.0
WBC ($10^3/\mu l$)				
Control	13.8 ± 0.4	15.4 ± 1.4	15.3 ± 0.9	13.5 ± 0.9
EPO(0)	12.6 ± 0.6	14.0 ± 1.1	14.4 ± 0.3	12.3 ± 1.4
EPO(6h)	12.6 ± 0.8	15.6 ± 1.1	13.9 ± 1.0	12.0 ± 0.8
EPO(1wk)	13.1 ± 0.8	14.8 ± 1.2	13.3 ± 0.4	12.9 ± 0.8
Platelet ($10^4/mm^3$)				
Control	27.3 ± 2.0	26.5 ± 1.9	28.4 ± 1.2	26.2 ± 2.0
EPO(0)	28.5 ± 2.0	26.8 ± 4.3	27.0 ± 3.4	28.2 ± 1.8
EPO(6h)	26.9 ± 0.9	27.0 ± 1.4	26.1 ± 1.8	26.1 ± 1.5

Data are presented as mean ± SEM (n = 7 to 8).
EPO = erythropoietin; WBC = white blood cell.

Table 2. Time Course of Changes in Plasma VEGF Levels

Groups	n	Baseline	6 Hours	1 Week	2 Weeks
VEGF (pg/ml)					
Control	4	<9.0	22.5 ± 3.3*	<9.0	<9.0
EPO(0)	4	<9.0	21.6 ± 5.0*	<9.0	<9.0

Data are presented as mean ± SEM. *p < 0.05 vs. baseline.
EPO = erythropoietin; VEGF = vascular endothelial growth factor.

JACC Vol. 48, No. 1, 2006
July 4, 2006:176–84

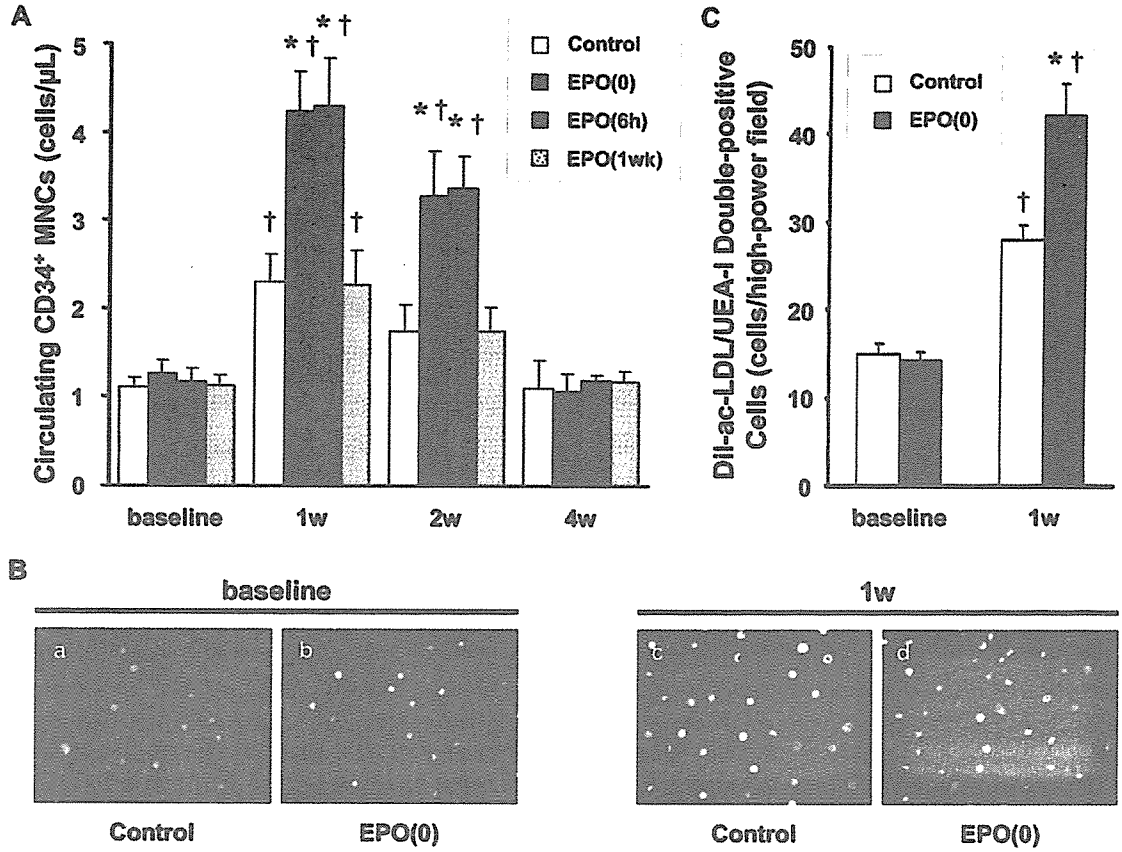

Figure 4. **(A)** Time course of changes in circulating CD34+MNC count after left anterior descending coronary artery (LAD) ligation in different experimental groups. **(B)** Representative images of double-stained cultured cells (1,1′-dioctadecyl-3,3,3′,3′-tetramethylindocarbocyanine-labeled acetylated low density lipoprotein [Dil-ac-LDL] and *Ulex europaeus* agglutinin I [UEA-I]) at baseline **(a, b)** and 1 week after LAD ligation **(c, d)** from dogs with and without erythropoietin (EPO) treatment immediately after LAD ligation. **(C)** Quantitative analysis of endothelial progenitor cell culture assay. *$p <$ 0.05 vs. the control group. †$p < 0.05$ vs. baseline.

EPO(1wk) group. Furthermore, the administration of EPO 1 week after the LAD ligation did not affect the number of CD34+MNCs at any given time point.

In the culture assay of MNCs, the number of Dil-ac-LDL/UEA-I double-positive cells obtained from blood 1 week after MI increased compared with that at baseline in both control and EPO(0) groups. Importantly, the double-positive cell number obtained from blood 1 week after MI in the EPO(0) group was significantly higher than in the control group (Figs. 4B and 4C).

Capillary density and regional MBF. Figure 5A shows the representative immunohistologic findings in the non-ischemic (panels a to d) and ischemic (panels e to h) regions at 4 weeks after MI. In the nonischemic region, there was no difference in the capillary density and capillary-to-myocyte ratio when comparing groups. In the ischemic region, the capillary-to-myocyte ratio as well as capillary density was significantly higher in the EPO(0) and EPO(6h) groups, but not in the EPO(1wk) group, than in the control group (Figs. 5B to 5C).

Figure 6 shows the changes in regional MBF in the ischemic regions in different experimental groups. There was no significant difference in MBF at 90 min when comparing experimental groups. At 4 weeks after MI, MBF was more increased in the EPO(0) and EPO(6h) groups, but not in the EPO(1wk) group, than in the control group.

Effects of immediate or delayed EPO treatment on cardiac function and infarct size. Throughout the experimental protocols, there was no difference in either ABP or HR when comparing the groups (Table 3).

Figure 7 shows the time course of changes in LVEF (panel A), LVEDD (panel B), and LVEDP (panel C) in different experimental groups. There were no significant differences in baseline LVEF, LVEDD, and LVEDP when comparing the groups.

Ninety minutes, 1 week, and 4 weeks after MI, LVEF was higher in the EPO(0) group than in the other groups. Ninety minutes and 1 week after MI, there was no difference in LVEF when comparing the EPO(6h) group and the control group. When comparing the time points of 1 week and 4 weeks after MI, LVEF decreased in the control and the EPO(1wk) groups but not in the EPO(6h) group. One and 4 weeks after MI, LVEDD was lower in the EPO(0) group than in the other groups. When comparing the time points of 1 week and 4 weeks after MI, LVEDD increased in the control and EPO(1wk) groups but not in the EPO(6h) group. Ninety minutes after MI, LVEDP was lower in the

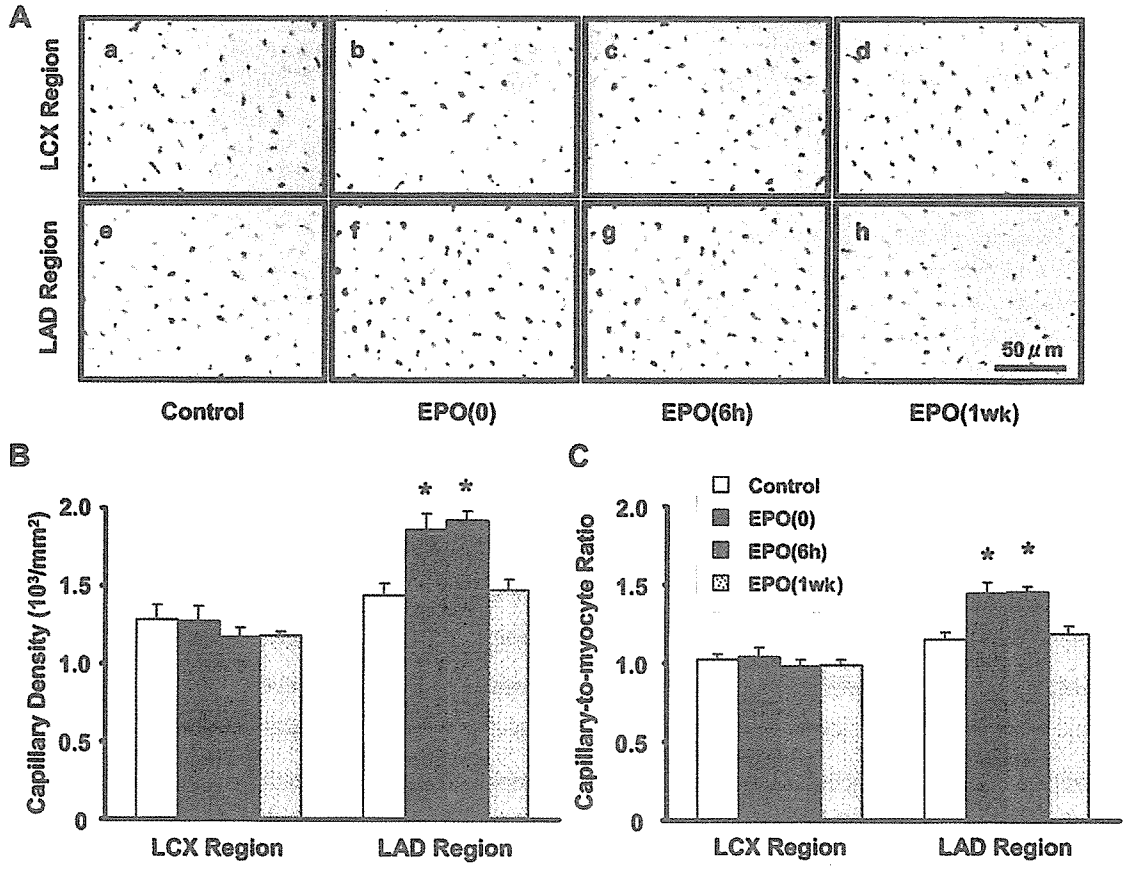

Figure 5. **(A)** Representative immunohistologic staining with an antibody against von Willebrand factor in nonischemic (left circumflex coronary artery [LCX]) **(a, b, c, d)** and ischemic (left anterior descending coronary artery [LAD]) **(e, f, g, h)** regions in different experimental groups. Capillary density **(B)** and capillary-to-myocyte ratio **(C)** of nonischemic (LCX) and ischemic (LAD) regions in different experimental groups. *$p < 0.05$ versus the control group. Abbreviations as in Figure 1.

EPO(0) group than in the other groups. Four weeks after MI, LVEDP was lower in the EPO(0) and EPO(6h) groups than in either the control or the EPO(1wk) group.

Myocardial infarct size 4 weeks after MI was smaller in the EPO(0) group than in the control group, although EPO treatment, initiated 6 h and 1 week after MI, did not reduce infarct size (Fig. 7D).

DISCUSSION

The present study showed that EPO administered 6 h after LAD ligation increased circulating CD34+MNCs, capillary density, MBF in the ischemic region, and prevented the worsening of cardiac function without reducing infarct size. The EPO enhances neovascularization, likely via EPC mobilization, and improves cardiac dysfunction in the chronic phase, although EPO has time-window limitations.

We showed that the EPO treatment immediately after the LAD ligation reduced infarct size, which is consistent with observations of previous reports (5–8). Because the infarct size-limiting effects of EPO appear rapidly, the nonerythroid effects of EPO, such as antiapoptosis and radical scavenging (4–8), may contribute to the reduction of infarct size.

Recent reports have shown that circulating CD34+MNC count correlated with EPC number in MNCs culture assay, and both increased at 1 to 2 weeks after EPO administration in animals and humans (9–11). In the culture assay, the number of Dil-ac-LDL/UEA-I double-positive cells obtained from blood at baseline did not differ between the two groups. The number of double-positive cells obtained from blood at 1 week after MI significantly increased compared with that at baseline in the control and EPO(0) groups. Further, the double-positive cell number obtained from blood in the EPO(0) group was higher than in the control group. These findings suggest that EPO augments increases in the number of MNCs that can differentiate into Dil-ac-LDL/UEA-I double-positive cells, an indicator of endothelial cells. Increases in the number of both CD34-positive cells and Dil-ac-LDL/UEA-I double-positive cells strongly suggest that EPO promotes EPC mobilization. The number of CD34+MNCs increased 1 week after MI in the canine model, which is consistent with observations from studies of patients with acute MI (21,22). Furthermore, the number of CD34+MNCs was higher in the EPO(0) and EPO(6h) groups than in the control group. This finding suggests that a single dose of EPO was effective in increasing the number of circulating EPCs after MI. Interestingly,

JACC Vol. 48, No. 1, 2006
July 4, 2006:176–84

EPO administered 1 week after MI failed to produce the identical effect, suggesting that EPO has a time window for promotion of EPC mobilization. We found that plasma VEGF levels were elevated, peaking at 6 h after MI and returned to the baseline 1 week after MI. The EPO did not affect plasma VEGF levels. Because both VEGF and EPO are known to promote EPC mobilization in experimental conditions and are independent predictors for the number of circulating EPCs in patients with coronary heart disease (9–11,23), they may additionally or synergistically contribute to EPC mobilization. Thus, it is likely that EPO alone, at least at the dose used in the present study, might not be enough to promote CD34+MNC mobilization 1 week after MI when VEGF returns to the baseline. Although we only investigated the low dose of EPO to consider the clinical implication, it is possible that high doses of EPO would show the different results. Further investigations are needed to clarify the mechanism of EPO-stimulated EPC mobilization.

The present study also showed that EPO increased capillary-to-myocyte ratio corrected for LV hypertrophy as well as capillary density in the EPO(0) and EPO(6h) groups, suggesting that EPO promotes the neovascularization in the ischemic region. Investigators have also reported that EPO enhances neovascularization in the ischemic region in the hind-limb occlusion model (9). As suggested in the present study, EPO may enhance neovascularization via EPC mobilization. Indeed, bone marrow-derived EPCs incorporate into foci of neovascularization at the border zone of MI (12,13), and administration of ex vivo-expanded EPCs resulted in increased myocardial neovascularization (24,25). In a rat stroke model, Wang et al. (26) showed that EPO treatment, initiated 24 h after MI, enhances angiogenesis. In addition, van der Meer et al. (27) showed that capillary density was increased in the rat post-MI model even when EPO was administered 3 weeks after MI. In contrast, we showed that EPO administered 1 week after MI failed to increase capillary density. The possible explanation for this discrepancy is attributable to the different doses of EPO used. In the studies by Wang et al. (26) (5,000 IU/kg for 7 days) and van der Meer et al. (27) (8,000 IU/kg every 3 weeks), relatively high doses of EPO were administered. In contrast, in the present study, a relatively low dose (1,000 IU/kg) of EPO was administered with a single injection, and the reason for this dose in the present study is for the possible translation of our results to clinical settings more easily (6), because 8,000 or 5,000 IU/kg EPO may cause side effects. On the other hand, we noticed that a higher dose of EPO would increase capillary density and improve the cardiac function even by the late administration of EPO for clinical use.

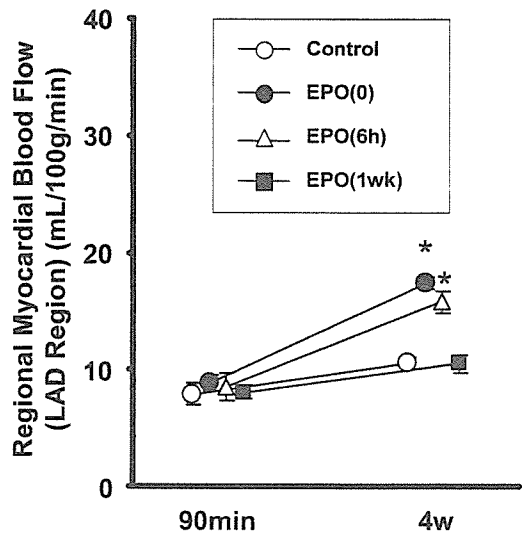

Figure 6. Regional myocardial blood flow in the ischemic (left anterior descending coronary artery [LAD]) region 90 min and 4 weeks after myocardial infarction in different experimental groups. *$p < 0.05$ versus the control group. EPO = erythropoietin.

Table 3. Time Course of Changes in Hemodynamic Parameters

Parameters	Baseline	90 Min	4 Weeks
ABP (mm Hg)			
Control	99 ± 3	101 ± 3	103 ± 2
EPO(0)	102 ± 3	99 ± 3	102 ± 2
EPO(6h)	101 ± 1	98 ± 2	101 ± 1
EPO(1wk)	102 ± 2	102 ± 3	103 ± 2
HR (per min)			
Control	131 ± 6	135 ± 6	129 ± 6
EPO(0)	128 ± 6	131 ± 3	131 ± 5
EPO(6h)	130 ± 7	135 ± 7	126 ± 6
EPO(1wk)	128 ± 6	128 ± 3	126 ± 6

Data are presented as mean ± SEM (n = 7 to 8).
ABP = arterial mean blood pressure; EPO = erythropoietin; HR = heart rate.

In the present study, MBF in the ischemic region was increased in both the EPO(0) and the EPO(6h) groups. Because neovascularization was also enhanced in these groups, increased MBF may occur secondary to the enhanced neovascularization.

The present study also showed that an administration of EPO immediately after the LAD ligation improved cardiac function at 90 min after MI, likely because of infarct size reduction, and subsequently prevented the development of cardiac dysfunction in the chronic phase. Because the previous reports showed that myocardial necrosis progresses within 6 h after the onset of MI (28,29), EPO was administered at time points of 6 h and later after LAD ligation to determine whether its activity is directed toward the acute phase of MI or the chronic phase of cardiac dysfunction. One week after MI, LVEF, LVEDD, or LVEDP was similar among the EPO(6h), EPO(1wk), and control groups. However, EPO administered 6 h, but not 1 week, after the LAD ligation improved cardiac dysfunction 4 weeks after MI when compared with the control group. Because we did not find any difference in infarct size at 4 weeks after MI between the EPO(6h) and the EPO(1wk) groups, the improvement of cardiac function in the EPO(6h) group was not attributable to the reduction of infarct size, but to the increased blood flow to the ischemic regions.

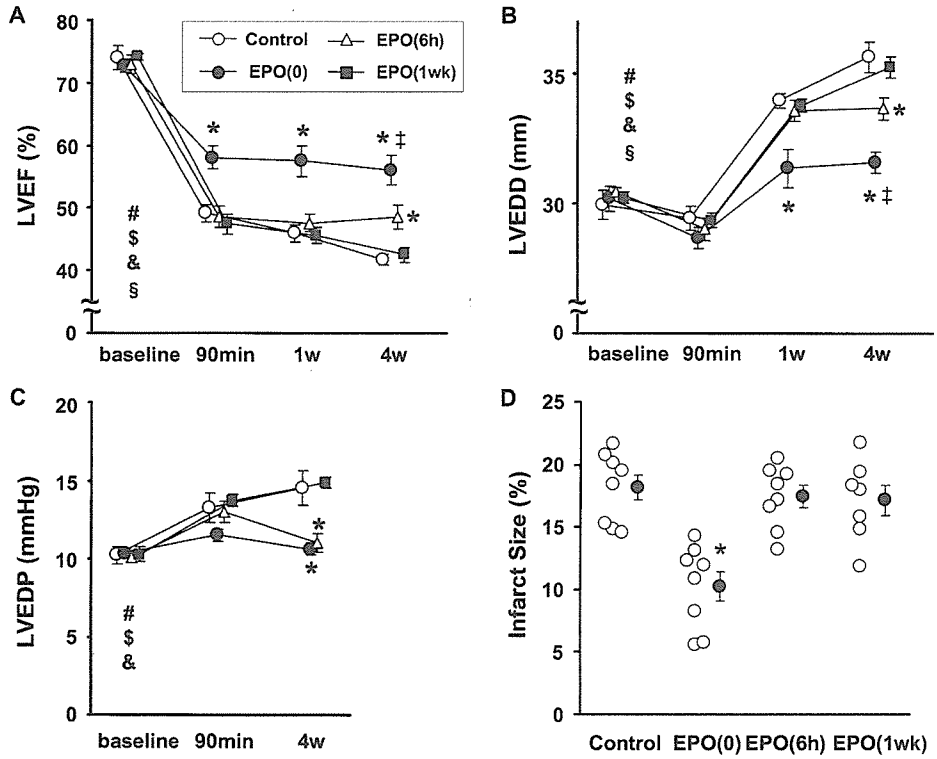

Figure 7. The time course of changes in left ventricular ejection fraction (LVEF) **(A)**, left ventricular end-diastolic dimension (LVEDD) **(B)**, and left ventricular end-diastolic pressure (LVEDP) **(C)** in different experimental groups. Statistically significant ($p < 0.05$) group-by-time interactions (analysis of variance for repeated measurements) are indicated by the following: # = all groups; $ = control × EPO(0) group; & = control × EPO(6h) group; § = EPO(0) × EPO(6h) group. **(D)** Infarct size at 4 weeks after myocardial infarction in different experimental groups. **Open circles** = infarct size in each animal. *$p < 0.05$ versus the control group. EPO = erythropoietin.

In conclusion, in addition to its acute effect on infarct size reduction, EPO may exert chronic cardioprotective effects through neovascularization and may be a useful adjunct for the treatment of patients with myocardial infarction.

Acknowledgments

The authors thank Hiroko Okuda, Akiko Ogai, Yoko Nagamachi, and Nobuko Kawasaki for their technical assistance.

Reprint requests and correspondence: Dr. Tetsuo Minamino, Department of Cardiovascular Medicine, Osaka University Graduate School of Medicine, 2-2 Yamadaoka, Suita, Osaka 565-0871, Japan. E-mail: minamino@medone.med.osaka-u.ac.jp.

REFERENCES

1. Krantz SB. Erythropoietin. Blood 1991;77:419–34.
2. Cotter DJ, Thamer M, Kimmel PL, Sadler JH. Secular trends in recombinant erythropoietin therapy among the U.S. hemodialysis population: 1990–1996. Kidney Int 1998;54:2129–39.
3. Sakanaka M, Wen TC, Matsuda S, et al. In vivo evidence that erythropoietin protects neurons from ischemic damage. Proc Natl Acad Sci U S A 1998;95:4635–40.
4. Chattopadhyay A, Choudhury TD, Bandyopadhyay D, Datta AG. Protective effect of erythropoietin on the oxidative damage of erythrocyte membrane by hydroxyl radical. Biochem Pharmacol 2000;59:419–25.
5. Moon C, Krawczyk M, Ahn D, et al. Erythropoietin reduces myocardial infarction and left ventricular functional decline after coronary artery ligation in rats. Proc Natl Acad Sci U S A 2003;100:11612–7.
6. Hirata A, Minamino T, Asanuma H, et al. Erythropoietin just before reperfusion reduces both lethal arrhythmias and infarct size via the phosphatidylinositol-3 kinase-dependent pathway in canine hearts. Cardiovasc Drugs Ther 2005;19:33–40.
7. Parsa CJ, Matsumoto A, Kim J, et al. A novel protective effect of erythropoietin in the infarcted heart. J Clin Invest 2003;112:999–1007.
8. Lipsic E, van der Meer P, Henning RH, et al. Timing of erythropoietin treatment for cardioprotection in ischemia/reperfusion. J Cardiovasc Pharmacol 2004;44:473–9.
9. Heeschen C, Aicher A, Lehmann R, et al. Erythropoietin is a potent physiologic stimulus for endothelial progenitor cell mobilization. Blood 2003;102:1340–6.
10. Bahlmann FH, DeGroot K, Duckert T, et al. Endothelial progenitor cell proliferation and differentiation is regulated by erythropoietin. Kidney Int 2003;64:1648–52.
11. Bahlmann FH, De Groot K, Spandau JM, et al. Erythropoietin regulates endothelial progenitor cells. Blood 2004;103:921–6.
12. Asahara T, Masuda H, Takahashi T, et al. Bone marrow origin of endothelial progenitor cells responsible for postnatal vasculogenesis in physiological and pathological neovascularization. Circ Res 1999;85:221–8.
13. Asahara T, Murohara T, Sullivan A, et al. Isolation of putative progenitor endothelial cells for angiogenesis. Science 1997;275:964–7.
14. Kitakaze M, Hori M, Morioka T, et al. Alpha 1-adrenoceptor activation mediates the infarct size-limiting effect of ischemic preconditioning through augmentation of 5′-nucleotidase activity. J Clin Invest 1994;93:2197–205.
15. Koumegawa J, Kawahara J, Kubo K, et al. Recombinant human erythropoietin corrects anemia of blood loss: a study in the dog. Int J Cell Cloning 1990;8:97–106.
16. Clifford CA, Hughes D, Beal MW, et al. Plasma vascular endothelial growth factor concentrations in healthy dogs and dogs with hemangiosarcoma. J Vet Intern Med 2001;15:131–5.
17. Horrigan MC, MacIsaac AI, Nicolini FA, et al. Reduction in myocardial infarct size by basic fibroblast growth factor after

temporary coronary occlusion in a canine model. Circulation 1996;94:1927–33.
18. Pu Q, Larouche I, Schiffrin EL. Effect of dual angiotensin converting enzyme/neutral endopeptidase inhibition, angiotensin converting enzyme inhibition, or AT1 antagonism on coronary microvasculature in spontaneously hypertensive rats. Am J Hypertens 2003;16:931–7.
19. Mori H, Haruyama S, Shinozaki Y, et al. New nonradioactive microspheres and more sensitive x-ray fluorescence to measure regional blood flow. Am J Physiol 1992;263:H1946–57.
20. Holm S. A simple sequentially rejective multiple test procedure. Scand J Stat 1979;6:65–70.
21. Shintani S, Murohara T, Ikeda H, et al. Mobilization of endothelial progenitor cells in patients with acute myocardial infarction. Circulation 2001;103:2776–9.
22. Massa M, Rosti V, Ferrario M, et al. Increased circulating hematopoietic and endothelial progenitor cells in the early phase of acute myocardial infarction. Blood 2005;105:199–206.
23. Asahara T, Takahashi T, Masuda H, et al. VEGF contributes to postnatal neovascularization by mobilizing bone marrow-derived endothelial progenitor cells. Embo J 1999;18:3964–72.
24. Kocher AA, Schuster MD, Szabolcs MJ, et al. Neovascularization of ischemic myocardium by human bone-marrow-derived angioblasts prevents cardiomyocyte apoptosis, reduces remodeling and improves cardiac function. Nat Med 2001;7:430–6.
25. Kawamoto A, Gwon HC, Iwaguro H, et al. Therapeutic potential of ex vivo expanded endothelial progenitor cells for myocardial ischemia. Circulation 2001;103:634–7.
26. Wang L, Zhang Z, Wang Y, Zhang R, Chopp M. Treatment of stroke with erythropoietin enhances neurogenesis and angiogenesis and improves neurological function in rats. Stroke 2004;35:1732–7.
27. van der Meer P, Lipsic E, Henning RH, et al. Erythropoietin induces neovascularization and improves cardiac function in rats with heart failure after myocardial infarction. J Am Coll Cardiol 2005;46:125–33.
28. Reimer KA, Lowe JE, Rasmussen MM, Jennings RB. The wavefront phenomenon of ischemic cell death. 1. Myocardial infarct size vs duration of coronary occlusion in dogs. Circulation 1977;56:786–94.
29. Hirayama A, Adachi T, Asada S, et al. Late reperfusion for acute myocardial infarction limits the dilatation of left ventricle without the reduction of infarct size. Circulation 1993;88:2565–74.

Original Article

Angiotensin II Type 1 Receptor Blocker Prevents Atrial Structural Remodeling in Rats with Hypertension Induced by Chronic Nitric Oxide Inhibition

Hidetoshi OKAZAKI[1)-3)], Tetsuo MINAMINO[4)], Osamu TSUKAMOTO[4)], Jiyoong KIM[1)], Ken-ichiro OKADA[4)], Masafumi MYOISHI[1)-3)], Masakatsu WAKENO[1)-3)], Seiji TAKASHIMA[4)], Naoki MOCHIZUKI[1),3)], and Masafumi KITAKAZE[2)]

The prevalence of atrial fibrillation (AF) increases in patients with hypertension. Angiotensin II is involved in structural atrial remodeling, which contributes to the onset and maintenance of AF in paced animal models. We investigated the role of angiotensin II in atrial structural remodeling in rats with hypertension. Ten-week-old male Wistar-Kyoto rats were randomly divided into 4 groups: a control group (no treatment), an N^{ω}-nitro-L-arginine methyl ester (L-NAME) group (administered L-NAME, an inhibitor of nitric oxide synthase, 1 g/l in drinking water), an L-NAME+candesartan group (L-NAME plus candesartan—an angiotensin II receptor blocker (ARB)—at 0.1 mg/kg/day), and an L-NAME+hydralazine group (L-NAME plus hydralazine at 120 mg/l in drinking water). Eight weeks after treatment, the L-NAME group showed significantly higher systolic blood pressure than the control group (197±12 *vs.*138±5 mmHg, $p<0.05$). Candesartan or hydralazine with L-NAME reduced systolic blood pressure to baseline. Chronic inhibition of NO synthesis increased the extent of fibrosis and transforming growth factor-β expression in atrial tissue, and both of these effects were prevented by candesartan, but not by hydralazine. Cardiac hypertrophy and dysfunction were induced in the L-NAME group, and these effects were also prevented by candesartan, but not by hydralazine. In contrast, the decrease in thrombomodulin expression in the atrial endocardium in hypertensive rats was restored by candesartan and hydralazine. The ARB prevented atrial structural remodeling, a possible contributing factor for the development of AF, in the hearts of rats with hypertension induced by long-term inhibition of NO synthesis. (*Hypertens Res* 2006; 29: 277–284)

***Key Words*: angiotensin II type 1 receptor blocker, atrial fibrillation, nitric oxide, hypertension, atrial remodeling**

From the [1)]Department of Structural Analysis, National Cardiovascular Center Research Institute, Suita, Japan; [2)]Cardiovascular Division, National Cardiovascular Center, Suita, Japan; and [3)]Department of Bioregulatory Medicine and [4)]Department of Cardiovascular Medicine, Osaka University Graduate School of Medicine, Suita, Japan.

This study was supported by grants for research on Human Genome, Tissue Engineering, and Food Biotechnology (H13-Genome-11) and grants for Comprehensive Research on Aging and Health (H13-21seiki [seikatsu]-23) in Health and Labour Science Research from the Ministry of Health, Labour, and Welfare, Japan.

Address for Reprints: Tetsuo Minamino, M.D., Ph.D., Department of Cardiovascular Medicine, Osaka University Graduate School of Medicine, Suita 565–0871, Japan. E-mail: minamino@medone.med.osaka-u.ac.jp

Received September 7, 2005; Accepted in revised form January 13, 2006.

Introduction

Atrial fibrillation (AF) is associated with a high risk of cardiovascular morbidity and mortality, and its prevalence is expected to double in the next 50 years (*1–5*). Patients with hypertension and chronic heart failure (CHF) are at high risk of developing AF (*2*, *6*). The development and maintenance of AF are associated with changes in electrical and structural properties known as atrial remodeling (*7*, *8*). Kumagai *et al.* demonstrated that rapid atrial pacing caused electrical and structural atrial remodeling (*8*). Li *et al.* demonstrated that CHF induced by rapid ventricular pacing strongly promotes the induction of sustained AF by causing fibrosis, which is a mechanism different from that of AF related to atrial tachycardia (*7*, *9*). Importantly, both rapid atrial and ventricular pacing demonstrated that slowing of atrial conduction velocity is more important than shortening of the atrial effective refractory period in the development of AF, and that slowing of atrial conduction velocity is associated with extensive fibrosis (*8*, *9*). Thus, the prevention of atrial fibrosis is a promising strategy for the management of AF. Although atrial structural remodeling, a possible contributing factor for the development and maintenance of AF, is observed in atrial and ventricular rapid pacing models (*8*, *9*), it remains unknown whether it is involved in hypertensive hearts.

The renin-angiotensin system (RAS) is excessively activated in patients with CHF (*10–13*). Recent clinical data have clearly shown that the RAS suppression by treatment with an angiotensin-converting enzyme (ACE) inhibitor or an angiotensin type 1 receptor blocker (ARB) reduces the new onset of AF in patients with CHF (*14–16*). Consistent with the clinical data, RAS suppression by ACE inhibitors or ARBs prevents atrial structural remodeling in both rapid atrial and ventricular pacing models (*8*, *17*). Recently, an ARB has been shown to confer better protection against the new onset of AF in hypertensive patients with left ventricular (LV) hypertrophy compared with a β-adrenergic receptor antagonist (*18*), suggesting that angiotensin II may also play an important role in the onset and maintenance of AF in hypertension. In the present study, we examined the occurrence of atrial structural remodeling and the role of angiotensin II in its development using candesartan, an ARB, in the hearts of rats with hypertension induced by long-term inhibition of nitric oxide (NO) synthesis (*19*). Furthermore, since atrial endocardial dysfunction such as a reduced thrombomodulin (TM) expression was previously induced in a rapid atrial pacing model (*20*, *21*), we also investigated the effects of candesartan or hydralazine on TM expression in the atrium in this hypertensive model.

Methods

Materials

Candesartan was provided by Takeda Co., Ltd. (Osaka, Japan), and the other drugs were obtained from Sigma Chemical Co. (St. Louis, USA). All procedures were performed in conformity with the Guide for the Care and Use of Laboratory Animals (NIH publication No. 93–23, revised 1985) and approved by the Osaka University Ethical Committee for Laboratory Animal Use.

Animal Model of Chronic Inhibition of NO Synthesis

Since endothelial dysfunction has been documented in patients with CHF and hypertension (*22*, *23*), which is largely the result of a decrease in the bioavailability of NO (*24*, *25*), we adopted a hypertensive rat model induced by a long-term inhibition of NO synthesis. Ten-week-old male Wistar-Kyoto rats (Charles River, Yokohama, Japan) were randomly divided into 4 groups. The control group ($n=11$) received no treatment. The N^{ω}-nitro-L-arginine methyl ester (L-NAME) group ($n=11$) received L-NAME at 1 g/l in drinking water. The L-NAME+candesartan group ($n=11$) received L-NAME plus candesartan (0.1 mg/kg per day) orally. The L-NAME+hydralazine group received L-NAME plus hydralazine (120 mg/l in drinking water). Body weight (BW) was measured 1 week before and 8 weeks after the initiation of treatment. Blood pressure (BP) and heart rate (HR) were measured by the tail-cuff method 1 week before and 1, 2, 4, and 8 weeks after starting the experiments. All rats were housed, treated, and subjected to euthanasia as described previously (*26*).

Echocardiographic Studies

Transthoracic echocardiography was performed using a machine equipped with a 7.5 MHz transducer (ALOKA Co., Ltd., Tokyo, Japan) after 8 weeks of treatment. Rats were anesthetized intraperitoneally with ketamine (15 mg/kg) and xylazine (5 mg/kg) and subjected to echocardiographic study. We measured echocardiographic parameters including LV end-diastolic dimension (LVDd), LV end-systolic dimension (LVDs), LV fractional shortening (LVFS), and the ratio of early to late filling wave of transmitral pulse-wave Doppler velocity (*E*/*A*).

Histopathological and Immunohistochemical Analysis

Eight weeks after treatment, rats in each group were sacrificed for morphometric, immunohistochemical and biochemical analyses. Excised hearts were weighed, separated into atrial and ventricular sections, cut, and stained with hematoxylin-eosin (HE) solution and Masson trichrome solution, and left atrial sections were carefully scanned as described previously (*26*). Each section was scanned at ×200 magnification. For immunohistochemistry, paraffin sections (5 μm thick) were incubated overnight at 4°C with a rabbit polyclonal anti-

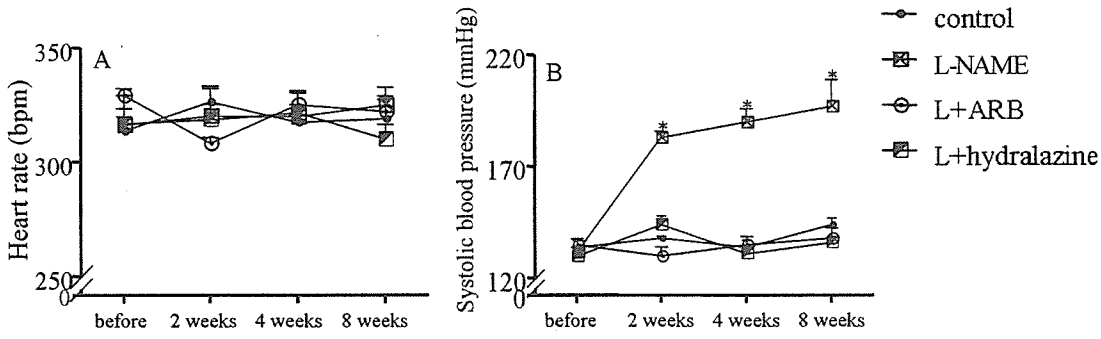

Fig. 1. *Hemodynamic parameters in groups tested. A: Heart rate. B: Systolic blood pressure. L-NAME,* N$^{\omega}$*-nitro-L-arginine methyl ester; L+ARB,* N$^{\omega}$*-nitro-L-arginine methyl ester plus angiotensin II receptor blocker; L+hydralazine,* N$^{\omega}$*-nitro-L-arginine methyl ester plus hydralazine. Data: mean±SEM.* *p < *0.05* vs. *control group.*

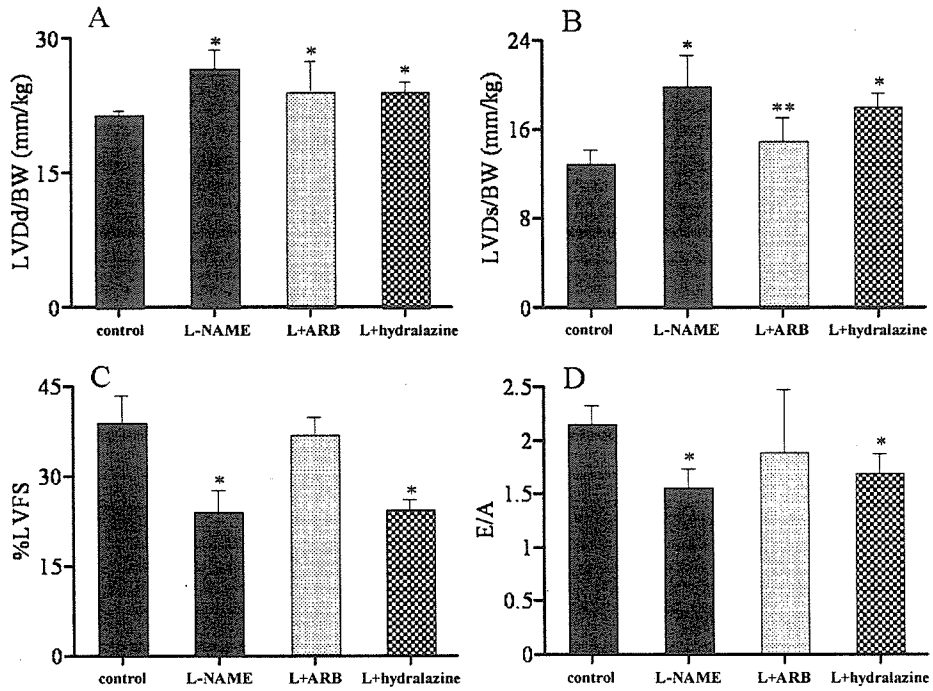

Fig. 2. *Echocardiographic parameters in groups tested. A: Left ventricular end-diastolic dimension (LVDd) corrected by body weight (BW). B: Left ventricular end-systolic dimension (LVDs)/BW. C: Left ventricular fractional shortening (LVFS). D:* E/A *ratio (ratio of early to late filling wave velocity). L-NAME,* N$^{\omega}$*-nitro-L-arginine methyl ester; L+ARB,* N$^{\omega}$*-nitro-L-arginine methyl ester plus angiotensin II receptor blocker; L+hydralazine,* N$^{\omega}$*-nitro-L-arginine methyl ester plus hydralazine. Data: mean±SEM.* *p < *0.05* vs. *control group,* **p < *0.05* vs. *L-NAME group.*

TM antibody (American Diagnostica Inc., Stamford, USA). A goat polyclonal anti-rabbit IgG antibody (DAKO) was used as a secondary reagent.

Real-Time Quantitative Reverse Transcriptase–Polymerase Chain Reaction

Reverse transcriptase–polymerase chain reaction (RT-PCR) of left atrial samples of rat was performed according to the Omniscript Reverse Transcription Handbook (QIAGEN Inc., Hilden, Germany). The rat primers and probes used for quantification of collagen type 1 and glyceraldehyde-3-phosphate-dehydrogenase (GAPDH) (internal control) were designed according to the manufacturer's protocol (Applied Biosystems, Foster City, USA) and those for transforming growth factor (TGF)-β were designed as described previously (*27*). Real-time quantitative RT-PCR was performed with an ABI PRISM7700 Sequence Detection System (Applied Biosys-

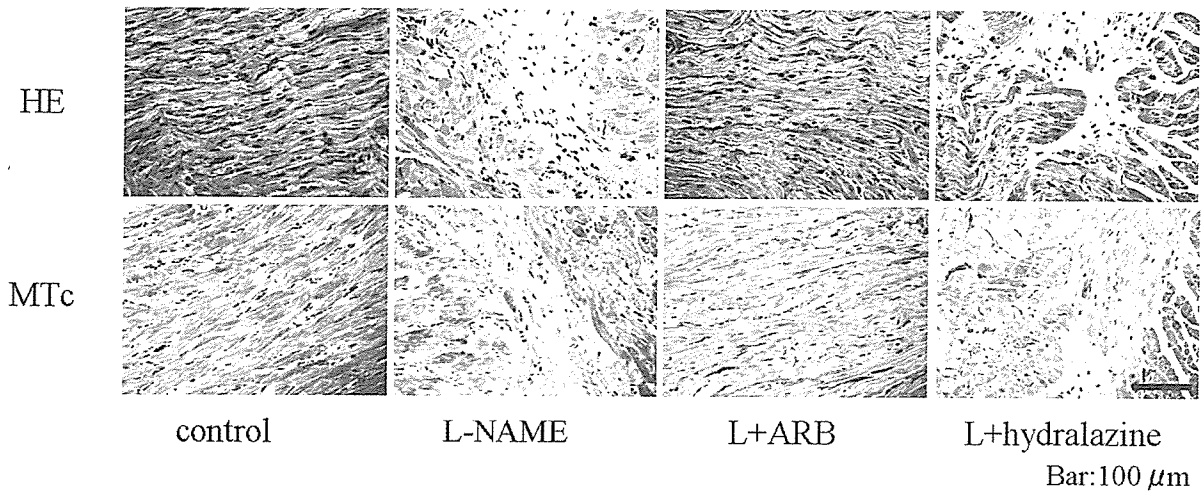

Fig. 3. *Effects of angiotensin II receptor blocker (ARB) on atrial structural remodeling in the hypertensive rat model. Atrial sections were stained with hematoxylin-eosin (HE) and Masson's-Trichrome (MTc). The bar indicates 100 μm. L-NAME,* N^{ω}*-nitro-L-arginine methyl ester; L+ARB,* N^{ω}*-nitro-L-arginine methyl ester plus angiotensin II receptor blocker; L+hydralazine,* N^{ω}*-nitro-L-arginine methyl ester plus hydralazine.*

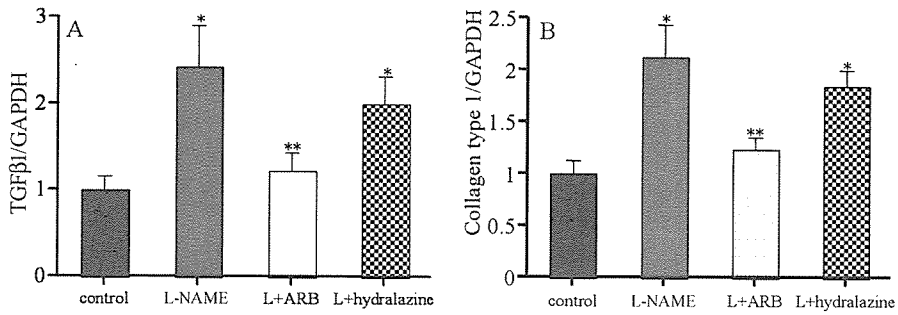

Fig. 4. *Expression of collagen type 1 and transforming growth factor (TGF)-β in atrial tissue in the hypertensive rat model. Each sample of TGF-β 1(A) and collagen type 1(B) was normalized by glyceraldehyde-3-phosphate-dehydrogenase (GAPDH). L-NAME,* N^{ω}*-nitro-L-arginine methyl ester; L+ARB,* N^{ω}*-nitro-L-arginine methyl ester plus angiotensin II receptor blocker; L+hydralazine,* N^{ω}*-nitro-L-arginine methyl ester plus hydralazine. Data: mean±SEM.* $^{*}p<0.05$ *vs. control group,* $^{**}p<0.05$ *vs. L-NAME group.*

tems) by the relative standard curve method. The target amount was determined from the relative standard curves constructed with serial dilutions of the control total RNA.

Immunoblot Analysis

Protein extraction and immunoblot analysis of left atrial samples of rats were performed as described previously (*20*), and immunoreactive bands were quantified by densitometry (Molecular Dynamics, Sunnyvale, USA).

Statistical Analysis

Data are expressed as the mean±SEM. Heart weight (HW), BW, hemodynamic variables, collagen type 1 or TGF-β expression normalized by GAPDH and TM protein levels were compared using one-way ANOVA followed by Bonferroni's test for multiple comparisons. Comparisons of the changes of BP among the groups over time were performed by two-way repeated-measures ANOVA followed by Bonferroni's correction, and values of $p<0.05$ were considered to be statistically significant.

Results

Hemodynamic Parameters

HR and systolic BP (SBP) are presented in Fig. 1. The HR was comparable among the 4 groups tested and did not change throughout the study. SBP was comparable among the

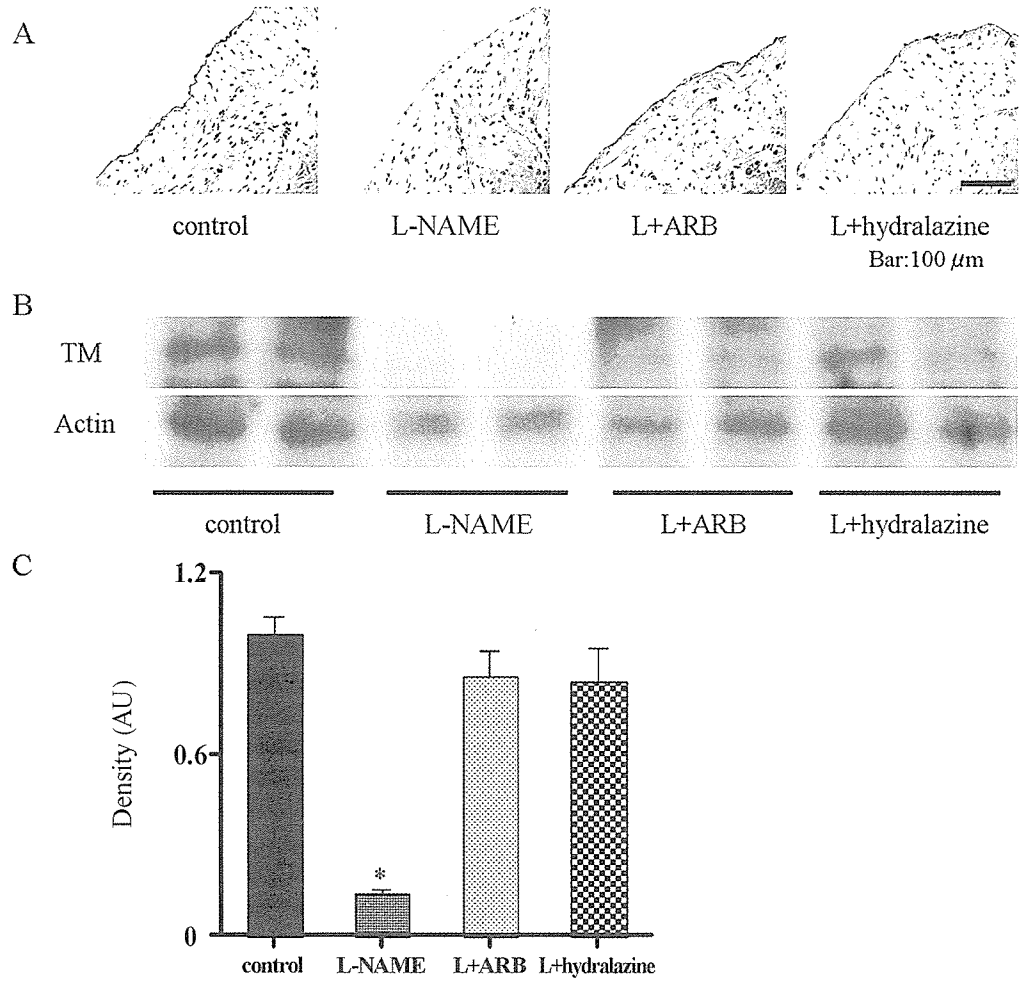

Fig. 5. *Thrombomodulin (TM) expression in atrial tissues in the hypertensive rat model. A: Representative changes of TM expression in the atrial endocardium. The bar indicates 100 μm. B: Immunoblot analysis for TM protein expression in each group tested. C: Quantitative analysis of TM protein expression. L-NAME,* N^{ω}*-nitro-L-arginine methyl ester; L+ARB,* N^{ω}*-nitro-L-arginine methyl ester plus angiotensin II receptor blocker; L+hydralazine,* N^{ω}*-nitro-L-arginine methyl ester plus hydralazine; AU, arbitrary unit. Data: mean±SEM.* *$p<0.05$ *vs. control group.* $N=3$.

4 groups before the study. In the L-NAME group, SBP increased progressively and became higher than that in the control group from 2 weeks of treatment onwards. The increase in SBP produced by L-NAME was decreased to the baseline by candesartan or hydralazine.

Effects of Candesartan and Hydralazine on Cardiac Hypertrophy and Dysfunction in Hypertensive Rats

The chronic treatment of rats with L-NAME significantly ($p<0.05$) increased the HW/BW ratio compared with that in the controls (3.50±0.05 *vs.* 2.89±0.02). This increase was prevented by candesartan (2.98±0.14), but not by hydralazine (3.38±0.07).

Quantitative echocardiographic data are presented in Fig. 2. Both LVDd/BW and LVDs/BW in the L-NAME group were significantly larger than in the control group. In the L-NAME group, LVFS was significantly decreased compared with that in the control group, indicating that systolic dysfunction was induced when NO synthesis was chronically inhibited. Candesartan, but not hydralazine, completely restored the reduction of LVFS by treatment with L-NAME. In addition, the *E/A* ratio in the L-NAME group was significantly decreased compared with that in the control group, indicating that diastolic dysfunction was also induced when NO synthesis was chronically inhibited. Candesartan, but not hydralazine, completely restored the reduction of *E/A* induced by L-NAME.

Effects of Candesartan and Hydralazine on Atrial Structural Remodeling in Hypertensive Rats

The extent of atrial fibrosis in the L-NAME group 8 weeks after treatment was significantly greater than that in the control group. This fibrotic change was prevented by candesartan, but not by hydralazine (Fig. 3). Quantitative analysis by real-time RT-PCR demonstrated that the mRNA levels of collagen type 1 and TGF-β in whole atrial tissue were significantly increased in the L-NAME group, while the increase in either molecule was reversed to the control levels by candesartan, but not by hydralazine (Fig. 4).

Hemodynamic Effects on TM Expression in the Atrium of Hypertensive Rats

Eight weeks after treatment by L-NAME, immunohistological analysis revealed that TM expression on the atrial endocardial surface was markedly decreased (Fig. 5A). Treatment with candesartan or hydralazine comparably reversed the decrease in atrial TM levels induced by chronic inhibition of NO synthesis (Fig. 5B, C).

Discussion

The present study demonstrated that candesartan, an ARB, but not hydralazine, prevented the progression of atrial fibrosis as well as LV hypertrophy and dysfunction in a hypertensive rat model induced by chronic inhibition of NO synthesis. Furthermore, candesartan and hydralazine comparably attenuated the reduction in TM expression in the atrial endocardium in this model. These findings suggest that angiotensin II plays an important role in the pathophysiology of atrial and ventricular structural remodeling in the hypertensive heart model. To our knowledge, the present study is the first to demonstrate a reduction of TM expression in left atrial tissue in hypertensive hearts.

Recent animal models of AF have proposed two principal forms of atrial remodeling: electrical remodeling, which affects cellular electrical properties, and structural remodeling, which alters the architecture of atrial tissue (*7–9*, *28*). Atrial tachycardias cause ionic remodeling while decreasing the atrial refractory period and promoting atrial reentry (*29*, *30*). By contrast, CHF produces extensive atrial interstitial fibrosis compared with atrial tachycardia, which promotes arrhythmogenesis by interfering with atrial conduction (*7*). Although Takemoto *et al.* clearly demonstrated that long-term inhibition of NO synthesis induces fibrotic changes in the left ventricle (*31*), the present study is the first to demonstrate structural atrial remodeling, a possible contributing factor for the development of AF, in the hypertensive heart model. Since we found extensive atrial fibrosis in this hypertension model, it is likely that the morphological changes in the atrium of hypertensive hearts are similar to those found in CHF rather than to those in atrial-tachycardia pacing. These morphological differences in atrial tissue may reflect a difference in the pathophysiology of atrial fibrosis.

Recent clinical trials have demonstrated a reduction in the development and recurrence of AF by ACE inhibitors and ARBs in patients with CHF and hypertension (*14*, *32*). Thus, the inhibition of the RAS is a novel concept for the prevention of AF that may target the underlying abnormalities of cardiac structure and electrical physiology that lead to AF. In the present study, candesartan, an ARB, but not hydralazine, prevented the progression of atrial fibrosis as well as LV hypertrophy and dysfunction in the hearts of hypertensive rats. There are two possible mechanisms by which candesartan prevented atrial structural remodeling in experimental hypertension with LV hypertrophy. One possible mechanism is the prevention of LV hypertrophy that may hemodynamically overload the atrium. LV hypertrophy is associated with a high incidence of AF in hypertensive patients (*6*). Thus, an antihypertensive drug, such as an ACE inhibitor or an ARB that can reverse LV hypertrophy, may effectively prevent the occurrence of AF (*33*). Indeed, in the LIFE study, an ARB, losartan, significantly reduced the incidence of AF compared with a β-adrenergic antagonist (*18*). The other possible mechanism is a direct anti-fibrotic effect of RAS inhibition. In both rapid atrial and ventricular pacing models, there are reports that the RAS inhibition by ACE inhibitors or ARB attenuates the development of atrial fibrosis that leads to the slowing of atrial conduction velocity (*8*, *9*). Candesartan, an ARB, may reduce the extent of atrial fibrosis due to reduction of LV hypertrophy as well as its direct antifibrotic effect in hypertensive hearts. Furthermore, it is likely that an inverse agonist effect by candesartan will be beneficial for preventing activation of angiotensin II type 1 receptor due to atrial stretch (*34*).

Consistent with these atrial morphological changes, quantitative analysis by real-time RT-PCR demonstrated that mRNA levels of collagen and TGF-β increased in this model. TGF-β is a cytokine known to play an important role in stimulating fibrosis (*35*). In a transgenic mouse model, constitutional activation of TGF-β produces atrial-restricted fibrosis and promotes inducibility of AF. Since angiotensin II induces the up-regulation of TGF-β that leads to cardiac fibrosis (*36*), the attenuation of TGF-β by the blockade of angiotensin II type 1 receptor may result in the reduction of fibrosis in atrial tissue.

Thrombin bound to endothelial TM cannot convert fibrinogen to fibrin or activate the anticoagulant protein C. Therefore, TM is considered to be a potent intrinsic anticoagulant factor (*37*), and the loss of TM in atria may lead to an increased risk of thromboembolism. In the hypertensive heart model induced by chronic inhibition of NO synthesis, we found that the expression of TM on the atrial endocardium was reduced. Interestingly, in contrast to the different effects of candesartan and hydralazine on atrial structural remodeling, candesartan and hydralazine comparably reduced systemic BP and restored the expression of TM. Thus, it is likely that atrial expression of TM is affected by hemodynamic fac-

tors such as systemic BP. However, we cannot deny the possibility that the local left atrial pressure may have been different, because the *E/A* ratios of the two groups were different. Since little is known about the modulators of TM expression, further investigation will be required into the mechanism by which the atrial expression of TM is regulated.

Patients with hypertension show endothelial dysfunction that may be largely attributable to reduced NO bioavailability (*23–25*). Thus, the hypertension model induced by long-term inhibition of NO synthesis will share the pathophysiology of patients with hypertension. We and other groups demonstrated that angiotensin II plays an important role in the development of LV fibrosis and cardiac inflammation in this model (*25, 26, 38*). However, the present study is the first to demonstrate the important role of angiotensin II in atrial remodeling in this hypertensive model. We must examine the role of angiotensin II in atrial structural remodeling in other hypertensive hearts.

A limitation of this study was that we did not demonstrate that atrial fibrosis in this hypertension model was associated with an increased vulnerability to AF or an increased incidence of AF. Future investigation will be required to check the relationship between atrial structural remodeling and the occurrence of AF in this hypertensive heart model.

In conclusion, atrial structural remodeling was observed in a hypertensive rat model. Blockade of angiotensin II type 1 receptor attenuated atrial fibrosis and the reduction in TM in the atrial endocardium. We need to consider pathophysiological atrial remodeling when we treat patients with hypertension.

Acknowledgements

We thank Mr. Hirofumi Yukawa (ALOKA Co., Ltd.) for echocardiographic assistance, Ms. Yukari Arino for secretarial work, and Ms. Hiroko Okuda and Ms. Yoko Nagamachi for technical assistance.

References

1. Benjamin EJ, Wolf PA, D'Agostino RB, Silbershatz H, Kannel WB, Levy D: Impact of atrial fibrillation on the risk of death: the Framingham Heart Study. *Circulation* 1998; **98**: 946–952.
2. Wang TJ, Larson MG, Levy D, *et al*: Temporal relations of atrial fibrillation and congestive heart failure and their joint influence on mortality: the Framingham Heart Study. *Circulation* 2003; **107**: 2920–2925.
3. Minamino T, Kitakaze M, Sanada S, *et al*: Increased expression of P-selectin on platelets is a risk factor for silent cerebral infarction in patients with atrial fibrillation: role of nitric oxide. *Circulation* 1998; **98**: 1721–1727.
4. Minamino T, Kitakaze M, Asanuma H, *et al*: Plasma adenosine levels and platelet activation in patients with atrial fibrillation. *Am J Cardiol* 1999; **83**: 194–198.
5. Minamino T, Kitakaze M, Sato H, *et al*: Plasma levels of nitrite/nitrate and platelet cGMP levels are decreased in patients with atrial fibrillation. *Arterioscler Thromb Vasc Biol* 1997; **17**: 3191–3195.
6. Verdecchia P, Reboldi G, Gattobigio R, *et al*: Atrial fibrillation in hypertension: predictors and outcome. *Hypertension* 2003; **41**: 218–223.
7. Li D, Fareh S, Leung TK, Nattel S: Promotion of atrial fibrillation by heart failure in dogs: atrial remodeling of a different sort. *Circulation* 1999; **100**: 87–95.
8. Kumagai K, Nakashima H, Urata H, Gondo N, Arakawa K, Saku K: Effects of angiotensin II type 1 receptor antagonist on electrical and structural remodeling in atrial fibrillation. *J Am Coll Cardiol* 2003; **41**: 2197–2204.
9. Shinagawa K, Li D, Leung TK, Nattel S: Consequences of atrial tachycardia-induced remodeling depend on the preexisting atrial substrate. *Circulation* 2002; **105**: 251–257.
10. Cohn JN, Ferrari R, Sharpe N, on behalf of an International Forum on Cardiac Remodeling: Cardiac remodeling—concepts and clinical implications: a consensus paper from an international forum on cardiac remodeling. *J Am Coll Cardiol* 2000; **35**: 569–582.
11. Schnee JM, Hsueh WA: Angiotensin II, adhesion, and cardiac fibrosis. *Cardiovasc Res* 2000; **46**: 264–268.
12. Weber KT, Brilla CG: Pathological hypertrophy and cardiac interstitium. Fibrosis and renin-angiotensin-aldosterone system. *Circulation* 1991; **83**: 1849–1865.
13. Tanemoto M, Abe T, Obara N, Abe M, Satoh F, Ito S: Successful treatment of severe hypertension with the combination of angiotensin converting enzyme inhibitor and angiotensin II receptor blocker. *Hypertens Res* 2003; **26**: 863–868.
14. Vermes E, Tardif JC, Bourassa MG, *et al*: Enalapril decreases the incidence of atrial fibrillation in patients with left ventricular dysfunction: insight from the Studies of Left Ventricular Dysfunction (SOLVD) trials. *Circulation* 2003; **107**: 2926–2931.
15. Maggioni AP, Latini R, Carson PE, *et al*: Valsartan reduces the incidence of atrial fibrillation in patients with heart failure: results from the Valsartan Heart Failure Trial (Val-HeFT). *Am Heart J* 2005; **149**: 548–557.
16. Miura S, Saku K, Karnik SS: Molecular analysis of the structure and function of the angiotensin II type 1 receptor. *Hypertens Res* 2003; **26**: 937–943.
17. Shi Y, Li D, Tardif JC, Nattel S: Enalapril effects on atrial remodeling and atrial fibrillation in experimental congestive heart failure. *Cardiovasc Res* 2002; **54**: 456–461.
18. Wachtell K, Lehto M, Gerdts E, *et al*: Angiotensin II receptor blockade reduces new-onset atrial fibrillation and subsequent stroke compared to atenolol: the Losartan Intervention for End Point Reduction in Hypertension (LIFE) study. *J Am Coll Cardiol* 2005; **45**: 712–719.
19. Egashira K, Ni W, Inoue S, *et al*: Pravastatin attenuates cardiovascular inflammatory and proliferative changes in a rat model of chronic inhibition of nitric oxide synthesis by its cholesterol-lowering independent actions. *Hypertens Res* 2000; **23**: 353–358.
20. Yamashita T, Sekiguchi A, Iwasaki YK, *et al*: Thrombomodulin and tissue factor pathway inhibitor in endocardium of rapidly paced rat atria. *Circulation* 2003; **108**: 2450–2452.
21. Li-Saw-Hee FL, Blann AD, Lip GY: A cross-sectional and

diurnal study of thrombogenesis among patients with chronic atrial fibrillation. *J Am Coll Cardiol* 2000; **35**: 1926–1931.
22. Kubo SH, Rector TS, Bank AJ, Williams RE, Heifetz SM: Endothelium-dependent vasodilation is attenuated in patients with heart failure. *Circulation* 1991; **84**: 1589–1596.
23. Panza JA, Quyyumi AA, Brush JE Jr, Epstein SE: Abnormal endothelium-dependent vascular relaxation in patients with essential hypertension. *N Engl J Med* 1990; **323**: 22–27.
24. Node K, Kitakaze M, Yoshikawa H, Kosaka H, Hori M: Reduced plasma concentrations of nitrogen oxide in individuals with essential hypertension. *Hypertension* 1997; **30**: 405–408.
25. Ribeiro MO, Antunes E, de Nucci G, Lovisolo SM, Zatz R: Chronic inhibition of nitric oxide synthesis. A new model of arterial hypertension. *Hypertension* 1992; **20**: 298–303.
26. Minamino T, Kitakaze M, Papst PJ, *et al*: Inhibition of nitric oxide synthesis induces coronary vascular remodeling and cardiac hypertrophy associated with the activation of p70 S6 kinase in rats. *Cardiovasc Drugs Ther* 2000; **14**: 533–542.
27. Kuwahara F, Kai H, Tokuda K, *et al*: Transforming growth factor-beta function blocking prevents myocardial fibrosis and diastolic dysfunction in pressure-overloaded rats. *Circulation* 2002; **106**: 130–135.
28. Hoit BD: Matrix metalloproteinases and atrial structural remodeling. *J Am Coll Cardiol* 2003; **42**: 345–347.
29. Yue L, Feng J, Gaspo R, Li GR, Wang Z, Nattel S: Ionic remodeling underlying action potential changes in a canine model of atrial fibrillation. *Circ Res* 1997; **81**: 512–525.
30. Cha TJ, Ehrlich JR, Zhang L, Nattel S: Atrial ionic remodeling induced by atrial tachycardia in the presence of congestive heart failure. *Circulation* 2004; **110**: 1520–1526.
31. Takemoto M, Egashira K, Usui M, *et al*: Important role of tissue angiotensin-converting enzyme activity in the pathogenesis of coronary vascular and myocardial structural changes induced by long-term blockade of nitric oxide synthesis in rats. *J Clin Invest* 1997; **99**: 278–287.
32. Cohn JN, Tognoni G: A randomized trial of the angiotensin-receptor blocker valsartan in chronic heart failure. *N Engl J Med* 2001; **345**: 1667–1675.
33. Dahlof B, Herlitz H, Aurell M, Hansson L: Reversal of cardiovascular structural changes when treating essential hypertension. The importance of the renin-angiotensin-aldosterone system. *Am J Hypertens* 1992; **5**: 900–911.
34. Zou Y, Akazawa H, Qin Y, *et al*: Mechanical stress activates angiotensin II type 1 receptor without the involvement of angiotensin II. *Nat Cell Biol* 2004; **6**: 499–506.
35. Border WA, Noble NA: Transforming growth factor beta in tissue fibrosis. *N Engl J Med* 1994; **331**: 1286–1292.
36. Kawano H, Do YS, Kawano Y, *et al*: Angiotensin II has multiple profibrotic effects in human cardiac fibroblasts. *Circulation* 2000; **101**: 1130–1137.
37. Esmon CT: The roles of protein C and thrombomodulin in the regulation of blood coagulation. *J Biol Chem* 1989; **264**: 4743–4746.
38. Takemoto M, Egashira K, Tomita H, *et al*: Chronic angiotensin-converting enzyme inhibition and angiotensin II type 1 receptor blockade: effects on cardiovascular remodeling in rats induced by the long-term blockade of nitric oxide synthesis. *Hypertension* 1997; **30**: 1621–1627.

Available online at www.sciencedirect.com
SCIENCE DIRECT®
Journal of Molecular and Cellular Cardiology 40 (2006) 666–674
Journal of Molecular and Cellular Cardiology
www.elsevier.com/locate/yjmcc

Blockade of histamine H_2 receptors protects the heart against ischemia and reperfusion injury in dogs

Hiroshi Asanuma [a], Tetsuo Minamino [b], Akiko Ogai [a], Jiyoong Kim [a], Masanori Asakura [a], Kazuo Komamura [a], Shoji Sanada [b], Masashi Fujita [b], Akio Hirata [b], Masakatsu Wakeno [a], Osamu Tsukamoto [a], Yoshiro Shinozaki [c], Masafumi Myoishi [a], Seiji Takashima [b], Hitonobu Tomoike [a], Masafumi Kitakaze [a,*]

[a] *Cardiovascular Division, National Cardiovascular Center, Suita, Suita City, Osaka Prefacture 565-8565, Tokai University School of Medicine, Isehara, Japan*
[b] *The Department of Internal Medicine and Therapeutics, Osaka University Graduate School of Medicine, Suita, Tokai University School of Medicine, Isehara, Japan*
[c] *Physiology Department, Tokai University School of Medicine, Isehara, Japan*

Received 15 September 2005; received in revised form 3 February 2006; accepted 8 February 2006
Available online 17 April 2006

Abstract

We have previously reported that histamine H_2 blockers may be cardioprotective in patients with chronic heart failure. Since both endogenous histamine and histamine H_2 receptors are present in heart tissue, we tested the hypothesis that the blockade of histamine H_2 receptors mediates protection against reversible or irreversible ischemia and reperfusion injury. In open-chest dogs, the left anterior descending coronary artery was occluded for 90 minutes, followed by reperfusion for 6 hours. Administration of famotidine and cimetidine from 10 minutes before occlusion until after 1 hour of reperfusion reduced infarct size ($17.0 \pm 4.1\%$ and $17.8 \pm 2.9\%$ vs. $36.9 \pm 5.9\%$ of the solvent group, respectively) Famotidine administration only during the reperfusion period for 1 hour also attenuated infarct size ($22.5 \pm 3.5\%$). There were no differences in either area at risk or collateral flow among the groups. In another set of experiments, we decreased coronary perfusion pressure in dogs so that the coronary blood flow decreased to 50% of the non-ischemic level. In such conditions, we observed the increases in histamine release compared with non-ischemic conditions (0.04 ± 0.03 to 0.28 ± 0.13 ng/ml, $p < 0.05$). Famotidine improved anaerobic myocardial metabolism gauged by both lactate extraction ratio and myocardial oxygen consumption. We conclude that the blockade of histamine H_2 receptors mediates improvements in the anaerobic myocardial metabolism, and thus protects against ischemia and reperfusion injury.

Keywords: Ischemia-reperfusion; Myocardial infarction; Coronary circulation; Histamine; Receptor pharmacology

1. Introduction

Histamine is one of the autacoids and provokes various cellular functions via the stimulation of four different G-protein-coupled receptors, i.e. histamine H_1–H_4 receptors [1,2]. Histamine H_2 receptors, in particular, are known to be located in gastric cells and contribute to the production of acids that may cause gastric ulcers [1,3]. Therefore, the blockade of histamine H_2 receptors has been developed as a drug for the treatment of gastric ulcers. Interestingly, we have previously reported that histamine H_2 blockers may be protective in patients with chronic heart failure (CHF) using the data mining technique [4], which enables us to find unexpected effective drugs for cardiovascular diseases [4]. In human ventricular tissue, histamine H_1 receptor expression was less abundant, whereas histamine H_2 receptors were highly expressed [5], and stimulation of H_2 receptors transduces the intracellular signals via the Gs protein, as well as beta receptors [2,6]. Indeed, it is reported that:

1. histamine produces a positive inotropic effect in human ventricular muscles, likely due to the exclusive activation of H_2 receptors [7,8];

* Corresponding author. Tel.: +81 6 6833 5012x2225; fax: +81 6 6836 1120.
E-mail address: kitakaze@zf6.so-net.ne.jp (M. Kitakaze).

0022-2828/$ - see front matter © 2006 Elsevier Ltd. All rights reserved.
doi:10.1016/j.yjmcc.2006.02.001

2. histamine exerts a positive chronotropic effect via the H_2 receptors [9];
3. and the blockade of histamine H_2 receptors decreases cardiac output in patients with CHF [10].

If these were the case, the blockade of histamine H_2 receptors protects the hearts against ischemia and reperfusion injury where histamine would be released in such a condition; beta-blockers are cardioprotective because catecholamine is released during ischemia and reperfusion.

We tested the hypothesis that the blockade of histamine H_2 receptors improves protection against ischemia and reperfusion injury in canine hearts. We also investigated whether histamine is released in response to ischemic stress and modulates the myocardial contractile and metabolic function in canine hearts with coronary hypoperfusion.

2. Materials and methods

2.1. Instrumentation

We have previously reported the details of the instrumentation procedure [11]. In brief, healthy adult beagle dogs for laboratory use (weighing 8–13 kg) were anesthetized with an intravenous injection of sodium pentobarbital (30 mg/kg), intubated, and ventilated using room air mixed with oxygen (100% O_2 at flow rate of 1.0–1.5 l/min). The arterial blood pH, pO_2, and pCO_2 before starting the protocol were 7.37 ± 0.03, 103 ± 4 and 37.9 ± 1.9 mmHg, respectively. The chest was opened through the left fifth intercostals space, and the heart was suspended in a pericardial cradle. The proximal portion of the left anterior descending coronary artery (LAD) was cannulated and perfused with blood via the left carotid artery through an extracorporeal bypass tube. Coronary perfusion pressure (CPP) was monitored at the tip of the coronary arterial cannula, and coronary blood flow (CBF) in the perfused region was measured with an electromagnetic flow probe attached to the bypass tube. A small, short collecting tube (diameter 1 mm, length 70 mm) was inserted into a small coronary vein near the center of the perfused region to sample coronary venous blood. The drained venous blood was collected in a reservoir placed at the level of the left atrium and was returned via the jugular vein. Left ventricular pressure was measured with a micromanometer (Konigsberg P-5) placed through the apex into the left ventricular cavity. Two pairs of ultrasonic crystals were placed on the inner one third of the myocardium 1 cm apart to measure the myocardial segmental length with an ultrasonic dimension gauge (Schuessler, 5 MHz). End-diastolic length (EDL) was determined at the R wave on the electrocardiogram, and end-systolic length (ESL) was determined at the minimum pressure differential. Then, fractional shortening (FS) was calculated as $[(EDL - ESL)/EDL] \times 100\%$. Agents were administered into the LAD via the bypass tube. To constitute the coronary bypass between the carotid artery and the LAD, less than 30 s interruption of the LAD was necessary, but we confirm that this brief period of ischemia does not provoke either myocardial injury or protection. This study conformed to the "Position of the American Heart Association on Research Animal Use" adopted by the Association in November 1984.

3. Experimental protocols

3.1. Protocol I: Effects of the histamine H_2 blocker on myocardial metabolism and coronary blood flow in ischemic hearts

After the hemodynamics stabilization, coronary arterial and venous blood were sampled for blood gas analysis, and for the measurement of histamine [12], lactate [13] and the end-product (NO_x) of nitric oxide (NO) levels [14,15]. The plasma histamine concentration was determined by the radioimmunoassay kit (SRL Co. Ltd.). Lactate extraction ratio (LER) was calculated as the coronary arterio-venous difference of the lactate concentration multiplied by 100 and divided by the arterial lactate concentration. Myocardial oxygen consumption ($M\dot{V}O_2$, ml/100 g per minute) was calculated as: CBF (ml/100 g per minute) × coronary arterial and venous blood oxygen difference (ml/dl).

To examine whether the administration of famotidine reduces the severity of myocardial ischemia, hemodynamic and metabolic parameters were monitored in 10 healthy adult beagle dogs. CPP was reduced so that CBF decreased to 50% of the baseline level for 5 min. After stabilization, either famotidine (16.7 μg/kg per min, an infusion rate of 0.0167 ml/kg per min at a concentration of 1.0 mg/ml, $N = 5$) or a solvent of famotidine (DMSO, 0.0167 ml/kg per minute, $N = 5$) was infused into the bypass tube for 20 min. After the measurements of hemodynamic parameters and blood samplings for the assessments of metabolic parameters, we quickly sampled endomyocardial tissue supplied by either LAD or left circumflex coronary artery (the non-ischemic area) into liquid nitrogen and stored it at –80 °C.

The famotidine was dissolved in DMSO before administration. A preliminary study showed that the dose of famotidine was the minimum dose required to cause maximum suppression of myocardial oxygen consumption without hemodynamic changes.

3.2. Methods for the measurements of plasma NO_x levels, and myocardial cyclic AMP and Gs protein levels

The method for the measurement of NO_x has been described previously [14,15]. Briefly, within 30 s of collection, heparinized blood was centrifuged for 5 min at 2000 × *g*. The plasma fraction was then diluted with an equal amount of nitrite/nitrate-free distilled water. Subsequently, 400 μl of diluted plasma was centrifuged at 200 × *g* through a micropore filter (Ultrafree MC Microcentrifuged Device, UFC3, Millipore, MA, USA) to remove substances larger than 10 kDa. The filtered plasma was analyzed using an automated procedure based on the Griess reaction. The amount of nitrite/nitrate within the sample was measured by its absorbance at 540 nm when mixed with the Griess reagent, 0.1% naphthylethlenediamide in 5%

H_3PO_4. The absorbance at 540 nm was also measured after passing the samples through a copper-plated cadmium column for nitrate reduction; this value expressed the total amount of plasma NO end-products (i.e. nitrate and nitrite). The cardiac NO level was defined as the differences in the level of the end-products of NO between coronary arterial and venous blood.

For the measurements of myocardial Gs protein levels, each frozen sample was homogenized mechanically in a homogenization buffer (20 mM Tris, 0.25 M sucrose, and 1 mM EDTA; pH 7.4), with a mechanical homogenizer. The homogenate was centrifuged at 600 × *g* for 5 minutes (4 °C) to remove nuclei and particulate cellular debris. A portion of the resulting supernatants was centrifuged at 250,000 × *g* for 1 hour to separate the membrane and cytosolic fractions. We measured Gs protein levels of the membrane fractions as previously reported [16] using a commercially available polyclonal antibody.

For the measurements of myocardial cyclic AMP (cAMP) levels, each sample of frozen muscle was homogenized mechanically in 500 ml of frozen hydrochloric acid (0.1 N) with a mechanical homogenizer. The homogenate was thawed and centrifuged at 5000 × *g* at room temperature for 15 minutes and the 100 ml aliquots of supernatant were subjected to the assay. Levels of cAMP were determined by a sensitive radioimmunoassay (cyclic AMP kit; Yamasa Shoyu Co., Choshi, Japan).

3.3. Protocol II: Effects of the histamine H_2 blockers on infarct size following 90 min of ischemia

In healthy adult beagle dogs, the bypass tube to the LAD was occluded for 90 min, followed by reperfusion for 6 hours, together with an intracoronary administration of famotidine (21.4 μg/kg per minute, an infusion rate of 0.0214 ml/kg per minute at a concentration of 1.0 mg/ml, famotidine group, $N = 6$), cimetidine (214 μg/kg per minute, an infusion rate of 0.0214 ml/kg per minute at a concentration of 10 mg/ml, cimetidine group, $N = 6$), promethazine (107 μg/kg per minute, an infusion rate of 0.0107 ml/kg per minute at a concentration of 5 mg/ml, promethazine group, $N = 6$) or the solvent (DMSO, 0.0214 ml/kg per minute, control group, $N = 6$) from 10 minutes before occlusion until after 1 hour of reperfusion. Promethazine is the selective antagonist of histamine H_1 receptors. Drugs were not infused during coronary occlusion. We also tested whether famotidine was effective when administered after the onset of reperfusion (famotidine after reperfusion). Famotidine (21.4 μg/kg per minute, an infusion rate of 0.0214 ml/kg per minute at a concentration of 1.0 mg/ml, $N = 6$) was infused into the bypass tube at the start of reperfusion for 1 hour of reperfusion (the famotidine (Rep) group). Hemodynamic parameters were monitored during myocardial ischemia and after the start of reperfusion. Infarct size was assessed 6 hours after the onset of reperfusion. A preliminary study showed that the doses of famotidine and cimetidine were the minimum doses required to cause the maximum infarct size-limiting effects without hemodynamic changes.

3.4. Measurements of infarct size and collateral blood flow

Six hours after the onset of reperfusion, while the LAD was reoccluded and perfused with autologous blood, Evans blue dye was injected into a systemic vein to identify the area at risk and the non-ischemic area in the hearts. The heart was then removed immediately, and sliced into serial transverse sections that were 6–7 mm in width. The non-ischemic area was defined as the tissue showing blue staining. The ischemic region was harvested and incubated at 37 °C for 20–30 minutes in 1% 2,3,5-triphenyltetrazolium chloride (TTC, Sigma Chemical Company) in 0.1 mol/l phosphate buffer adjusted to pH 7.4. TTC stains the non-infarcted myocardium a brick-red color, indicating the presence of a formazan product created through the reduction of TTC by dehydrogenases in viable tissues. In Protocol II, the area of myocardial necrosis and the area at risk were measured in all of the dogs on completion of the protocol by an operator who had no knowledge of the treatment given to each animal. Infarct size was expressed as a percentage of the area at risk.

Regional myocardial blood flow was determined as described previously [17]. Nonradioactive microspheres (Sekisui Plastic Co. Ltd., Tokyo, Japan) made of inert plastic were labeled with bromine (Br). The microspheres were administered 80 minutes after the start of coronary occlusion. The radio fluorescence of the stable heavy elements was measured with a wavelength dispersive spectrometer (PW 1480, Phillips Co. Ltd., Almelo, The Netherlands). Because the level of energy emitted is characteristic for specific elements, it was possible to quantify the radio fluorescence of the heavy element with which the microspheres were labeled. Myocardial blood flow was calculated according to the following formula: time flow = (tissue count) × (reference flow)/(reference count), and was expressed in milliliters per minute per gram wet weight. Endomyocardial blood flow was measured at the inner half of the LV wall.

3.5. Exclusion criteria

To ensure that all the animals used for analysis of infarct size in Protocol II were healthy and had been exposed to a similar extent of ischemia, the following standards were employed for the exclusion of unsatisfactory dogs: (1) subendocardial collateral blood flow greater than 15 ml/100 g per minute; (2) a heart rate greater than 170 beats/min; and (3) more than two consecutive attempts required to terminate ventricular fibrillation (VF) using low-energy DC pulses applied directly to the heart.

3.6. Statistical analysis

Statistical analysis was performed using ANOVA [18,19] to compare data among the groups. When ANOVA indicated a significant difference, paired data were compared using the Bonferroni test. Changes in the hemodynamic and metabolic parameters over time were assessed by ANOVA with repeated